



**FABRICATION and CHARACTERIZATION OF CdO THIN
FILMS: DIODE APPLICATIONS**

Harem Salih KADER

Master's Thesis

Physics department

Thesis Advisor: Assoc. Prof. Murat SOYLU

2017

All rights reserved

TR
BİNGÖL UNIVERSITY
INSTITUTE OF SCIENCE

**FABRICATION and CHARACTERIZATION OF CdO
THIN FILMS: DIODE APPLICATIONS**

MASTER'S THESIS

Harem Salih KADER

Institute Department : PHYSICS

Thesis Advisor : Assoc. Prof. Murat SOYLU

February 2017

TR
BİNGÖL UNIVERSITY
INSTITUTE OF SCIENCES

FABRICATION AND CHARACTERIZATION OF CdO THIN
FILMS : DIODE APPLICATIONS

MASTER'S THESIS

Harem Salih KADER

Institute Department : PHYSICS

This dissertation was accepted by the following committee on
17.02.2017 with the vote unity.

Prof. Şükrü KARATAŞ
Head of examining
committee

Assoc. Prof.
Murat SOYLU
Advisor

Assoc. Prof.
Nezir YILDIRIM
Member of examining
committee

I confirm the result above

Prof. İbrahim Y. ERDOĞAN
Director

PREFACE

To begin with, I thank (Allah) for his blessing who made me able to complete and perform this study with success. I would like to thank my supervisor, Assoc. Prof. Dr Murat SOYLU who does not spare his help and knowledge and gives the necessary support for the completion of my studies, during the course of the thesis.

I would like to thank Bingöl University Rector, the manager and staff of central laboratory for their support for the thesis work. I must express my very profound gratitude to my mother and members of my family for providing me with unfailing support and continuous encouragement throughout my years of study and through the process of researching and writing this thesis.

Thanks to the kind people from the city of Bingöl for their warm hospitality for me through two years in my study. I thank all those who assisted me in doing my work.

Harem Salih KADER

Bingöl 2017

CONTENT

PREFACE.....	i
CONTENT.....	ii
LIST OF SYMBOLS AND ABBREVIATIONS.....	iv
LIST OF FIGURES.....	vi
LIST OF TABLES.....	viii
ÖZET.....	ix
ABSTRACT.....	x
1. INTRODUCTION.....	1
2. LITERATURE REVIEW.....	3
3. MATERIAL AND METHOD.....	8
3.1. Experimental details.....	8
3.2. Sol-gel method.....	12
3.3. Thin film applications.....	12
3.4. Silicon.....	13
3.5. X-ray diffraction.....	14
3.6. Atomic force microscopy (AFM).....	14
3.7. Optical properties.....	14
3.8. Photoluminescence.....	16
3.9. Metal-semiconductor contacts.....	16
4. RESULT AND DISCUSSION.....	24
4.1. Structure, surface and optic properties.....	24
4.2. Electrical characteristics of CdO/p-Si heterojunction.....	29

REFERENCES.....	38
CURRICULUM VITAE.....	44



LIST OF SYMBOLS AND ABBREVIATIONS

R^*	: Richardson constant
e	: Electronic charge
E_g	: Band gap
E_c	: Conduction band minimum
E_f	: Fermi energy level
E_v	: Valance band maximum
$f(E)$: Fermi distribution function
k	: Boltzman constant
α	: Absorption coefficient
V	: Potential
V_b	: Built-in potential
ν	: Frequency
T	: Temperature
λ_g	: Photon wavelength
n	: Ideality factor
R	: Reflection
d	: Film thickness
I	: Net current at metal-semiconductor contact
I_0	: Saturation current at metal-semiconductor contact
V_{oc}	: Open-circuit voltage
$F(V)$: Norde function
R_s	: Series resistance
I_{min}	: Minimum current
V_{min}	: Minimum voltage
γ	: The dimensionless integer

Φ_b	: Schottky barrier height
Φ_m	: Work function of metal
h	: Planck constant
χ_s	: Electron affinity
A	: Absorbance
D	: particle size
J_{sc}	: short circuit current density
J_0	: saturation current density
R_{sh}	: shunt resistance
V_T	: thermal voltage
A^*	: Richardson constant
MS	: Metal-semiconductor
MIS	: Metal-insulating-semiconductor
I-V	: Current-voltage
FL	: Fermi level
SB	: Schottky barrier
MESFET	: Metal-semiconductor field effect transistor
TE	: Thermionic emission
TAE	: Thermionic field emission
FE	: Field emission
AFM	: Atomic force microscopy
PL	: Photoluminescence
XRD	: X ray diffraction
TCO	: Transparent conduction oxide
SEM	: Scanning electron microscope
CdO	: Cadmium oxide
et al.	: and others
Fig.	: Figure
vs.	: Versus

LIST OF FIGURES

Fig. 3.1.	Spin coating system.....	9
Fig. 3.2.	The basic steps of the sol-gel process.....	10
Fig. 3.3.	Atomic force microscopy (AFM) device.....	10
Fig. 3.4.	UV-vis spectrophotometer device	11
Fig. 3.5.	X-ray diffraction (XRD) device.....	11
Fig. 3.6.	Energy level diagram of a metal	17
Fig. 3.7.	Schematic structure of metal-semiconductor contact.....	17
Fig. 3.8.	The energy-band diagram of metal/p-type semiconductor rectifier contact.....	18
Fig. 3.9.	Metal/p-type semiconductor ohmic contact energy-band diagrams.....	19
Fig. 3.10.	p-n junction device under illumination and its symbol	20
Fig. 4.1.	XRD spectra of CdO thin film growth on glass substrate.....	24
Fig. 4.2.	AFM microphotograph in $40 \times 40 \mu\text{m}^2$ area of CdO thin film (inset shows the image of $5 \times 5 \mu\text{m}^2$ area)	26
Fig. 4.3.	(a) Transmittance, (b) absorbance and (c) reflectance spectra of CdO thin film.....	27
Fig. 4.4.	Plot of $(\alpha h\nu)^2$ vs. $h\nu$ for CdO thin film.....	28
Fig. 4.5.	PL spectra for CdO thin film.....	29
Fig. 4.6.	Energy band diagram of heterojunction	30
Fig. 4.7.	The forward and reverse bias semi-logarithmic $I-V$ characteristics of Al/CdO/p-Si heterojunction diode in dark and under various illumination intensities.....	31
Fig. 4.8.	Variation of barrier height vs. P for Al/CdO/p-Si heterojunction diode....	32

Fig. 4.9.	Variation of I_{ph} vs. P for Al/CdO/p-Si heterojunction diode.....	33
Fig. 4.10.	Current density-voltage characteristics at irradiance of 20, 40, 60 and 80 mW/cm ²	34
Fig. 4.11.	$I-V$ characteristics (open circle) with fitting curve (blue line) at irradiance of 80 mW/cm ² (Inset shows a diode equivalent circuit of device including diode and parasitic resistances).....	36
Fig. 4.12.	Plots of $F(V)$ vs. V	36



LIST OF TABLES

Table 4.1. Some structural and optic parameters of CdO thin film.....	25
Table 4.2. Illumination dependent values of various parameters determined from the $I-V$ characteristics of CdO/p-Si heterojunction.....	34



CdO İNCE FİLMLEİN FABRİKASYONU VE KARAKTERİZASYONU: DİYOT UYGULAMALARI

ÖZET

Katkısız CdO ince filmler sol-gel dönel kaplama yöntemi ile cam ve p tip Si altlıklar üzerine büyütüldü. X-ışını difraksiyon (XRD), ultraviolele-visible (UV/Vis) spektroskopisi ve atomik kuvvet mikroskobu materyalin yapısal, optik ve morfolojik özelliklerini araştırmak için kullanıldı. Elde edilen sonuçlardan kübik kristal yapı, nano parçacıklardan oluşan yüzey ve 2,29 eV'luk optik bant aralığı elde edildi. CdO/p-Si heteroeklem yapı, karanlık ve ışık şartları altında gerçekleştirilen akım-voltaj (I-V) ölçümleri ile doğrultucu ve fotodiyot özelliği gösterdi. Fotoakımın artan aydınlanma şiddeti ile arttığı gözlemlendi. CdO/p-Si heteroeklemi foto diyot özelliği gösterirken, 128 meV'luk açık devre voltaj (the open circuit voltage, V_{oc}) göstererek, güneş pili (solar cell) özelliğinin zayıf olduğu görüldü. CdO/p-Si heteroeklemi '1' den büyük idealite faktörü ile ideal olmayan diyot davranışı gösterdi. Bu durum arayüzey tabakasına, arayüzey hallerine ve seri dirence atfedildi. Sonuçlar CdO/p-Si heteroekleminin optoelektronik uygulamalarda bir fotodiyot olarak kullanılabileceğini gösteriyor.

Anahtar Kelimeler: Sol-gel büyütme, CdO ince film, diyot, elektriksel özellikler.

FABRICATION AND ELECTRICAL CHARACTERIZATION OF CdO THIN FILMS: DIODE APPLICATIONS

ABSTRACT

CdO thin films were deposited on p-Si and glass substrates by sol-gel spin coating method. X-ray diffraction (XRD), ultraviolet-visible (UV/Vis) spectrophotometer and atomic force microscopy (AFM) were used to investigate some properties of material. From these data, cubic crystal structure, surface consisting of nanoparticles and the band gap of 2.29 eV were confirmed, respectively. CdO/p-Si heterojunction shows rectifying and photodiode behavior, evaluating the current-voltage ($I-V$) characteristics in dark and under light. The photocurrent increases with increasing illumination intensity. While CdO/p-Si heterojunction shows photodiode property, solar cell performance needs to improve, showing the open circuit voltage (V_{oc}) of 128 meV. CdO/p-Si heterojunction diodes exhibited a non-ideal behavior with the ideality factor greater than unity that could be ascribed to the interfacial layer, interface states and series resistance. Results show that CdO/p-Si heterojunction can be used as a photodiode in the optoelectronic applications.

Keywords: Sol-gel growth, CdO thin film, diode, electrical properties.

1. INTRODUCTION

Thin film materials are an important place in our daily lives because of its many features. In our everyday lives, thin films in the semiconductor devices we use almost everywhere have a very important place. Optically transparent and electrically conductive thin films are important for the optoelectronic applications. Transparent family also includes materials such as graphene, polymers and carbon nanotubes (CNT). Semiconductor films are materials that are formed by arranging the atoms or molecules of the material to be coated using different production methods. Photovoltaics, liquid-crystal displays, OLEDs, touchscreens, electroluminescent display devices, solar cells based on transparent conducting films (TCFs) are attracting increasing attention. In the studies, films with a thickness of 1.5 μm are called thin films and big ones are called thick films. Today, semiconductor technology is one of the fundamental and determining elements of technological developments. Parallel to the developing technology, the field of use of thin films has been developing. Thin films are one of important components for the electronics and optoelectronic industry. Diodes and many devices are formed from thin layers of semiconductors or materials that exhibit electroluminescent properties. From computers to mobile phones, thin films have an important place in the making of devices that we often use in our daily lives. Thin films are also the basis of sensors used for medical, military and many other purposes. Semiconductor thin films are obtained by three basic methods. These are single-layered epitaxial (homoepitaxial) films, multilayered epitaxial (heteroepitaxial) films, and polycrystalline films. Homoepitaxial and heteroepitaxial films are costly films obtained by using advanced technology. In scientific studies; so that at a lower cost and practically obtained polycrystalline films are preferred. Polycrystalline films are grown on substrates such as large surface metal glass ceramic graphite. Due to its electrical and optical properties, they are semiconductor materials which have many applications such as solar cell, semiconductor photodetectors; that can be obtained by various methods.

CdO films are obtained by many methods. These include spraying, chemical vapor

deposition, ion implantation, sol-gel, atomic layer growth and chemical storage methods. In this study, CdO thin films were produced by sol-gel method. The sol-gel method is the easiest and cheapest method of obtaining thin films.

Sol-gel method is rather simple, more economic, suitable for intervention in the production process, no need for vacuum environment and step by step of production process and much more advantageous than other methods for the production of thin films. This method allows also p-type and n-type doping. In this study, first part is based on the general information about thin films. Second part is based on the previous studies on CdO thin films. Third part is based on materials to be used in the synthesis of CdO thin films and fabrication of CdO/p-Si heterojunction, general information about devices to be used to characterize the thin films. Fourth part is based on the analysis of experimental results, conclusion and contribution to literature.

2. LITERATURE REVIEW

To synthesize CdO thin films, there are many methods such as sol-gel (Mane et al. 2006), magnetron sputtering (Gurumurugan et al. 1996), DC-activated reactive evaporation (Sravani et al. 1991), pulsed laser deposition, (Varkey and Fort 1994), chemical bath deposition (Phatak and Lal 1994), spray pyrolysis, (Yan et al. 2001, Gurumurugan et al. 1995, Saravani et al. 1994). The Cd⁺ ions or oxygen vacancies produce donor states. In this case, CdO is n-type semiconductors. Burbano et al. (2011) reported that p-type CdO was not obtained, despite all growth conditions.

CdO thin films were prepared on glass bottoms using a new precursor solvating sol-gel technique based on Cd(OOCCH₃)₂.2H₂O, ethylene glycol, glycerol and triethylamine. The films were annealed at 200 °C in the open air atomic force microscope, X-ray diffraction and UV-VIS spectrophotometer were used. The CdO thin films obtained are of high quality polycrystalline and permeability at 95% for a wavelength of 600 nm, and almost 100% for a wavelength of 700 nm to 1100 nm. The indirect and direct band-gap energy values were estimated to be 2.06 and 2.59 eV, respectively. The resistances of the films were found to be $2 \times 10^2 \Omega\text{cm}$ (Carballeda-Galicia et al. 2000).

Rajput et al. (2017) reported a study on nano-cauliflower like structure of CdO thin film deposited by sol-gel method. In this study, samples were annealed at different temperatures from 350 °C to 650 °C. Scanning electron microscope (SEM) and X-ray diffraction (XRD) were used to investigate the surface morphology and crystal structure.

It has been seen that optical band gap decreases from 2.42 to 2.20 eV while the annealing temperature increases in from 350 °C to 550 °C. Furthermore, the current-voltage (I-V) characteristics of annealed CdO films were analysed. Annealing temperature affected the rectifying behavior and the electrical conductivity of annealed CdO film at 450 °C film was determined to be highest.

Structural and optical properties of CdO are varied by doping concentration. sol-gel method allows doping with different gallium concentrations of CdO thin films. A systematic study was performed on CdO thin films with various gallium concentrations (0.01 M, 0.03 M, 0.05 M, 0.07 M and 0.09 M). The existence and the chemical composition of Ga element were confirmed by X-ray photoelectron spectroscopy (XPS). The optical band gap of CdO film decreases as Ga-doping concentration increases. In order to investigate the surface morphology, The field emission scanning electron microscopy (FESEM) was used. The grain size of the CdO films was found due to gallium concentrations (Thambidurai et al. 2015).

Sonawane et al. (2017) fabricated room temperature LPG sensor based on the CdO thin films. Cd(OH)₂ nanowires were synthesized on the FTO coated glass substrate. After air annealing Cd(OH)₂ film at 290 °C, the surface has become necklace like nanostructure film. To form CdO based heterojunction, PbS nanoparticles were coated by using the successive ionic layer adsorption and reaction (SILAR) method. Thus, n-CdO/p-PbS nano-heterojunction device was fabricated, resulting p/n junction. The maximum response of 51.10% was obtained when exposed to 1176 ppm concentration of LPG. The charge transport was attributed to a mechanism in which the work function of PbS changed and the carrier density increased. By using CdO thin films as component layer, gas sensing applications may be developed.

There are many parameters that affect the properties of CdO thin films. A study was performed to investigate the effects of annealing on the optical and electrical properties of CdO thin films prepared by thermal evaporation. The investigated parameters were measured before annealing and after annealing. The annealing temperature was 500 °C for 1 h. The band gap energy varied slightly from 2.48 eV to 2.42 eV after annealing. From electrical measurement, it was seen that the resistivity decreased after annealing. This case was attributed to the increased carrier concentration. It has been confirmed that CdO thin films has n-type conductivity. A cubic crystal structure was determined from XRD data, indicating locally polycrystalline structure. Annealing also has an effect on grain size. The crystallinity of the CdO thin films showed improvement after annealing. A relationship was established between increasing grain size and decreasing band gap.

CdO thin films took the most important role in device construction. Taşcıoğlu et al. (2012) fabricated nanostructure CdO/p-GaAs by the sol-gel method. AFM images confirmed that CdO film coated onto GaAs substrate had nanoparticles. Al/CdO/p-GaAs heterijunction structure exhibited the rectifying behavior with the barrier height of 0.62 eV and ideality factor of 2.29. Electrical measurements of the diode were evaluated as the current-voltage and capacitance-conductance-voltage. Hill-Coleman method based on capacitance-voltage and conductance-voltage measurements was used to determine the energy distribution profiles of interface states. The order of interface state density was obtained to be $10^{12} \text{ eV}^{-1}\text{cm}^{-2}$. The deviation of ideal behavior was attributed to the series resistance and interface states.

A few black samples obtained as a result of temperature tests at 800 °C Cadmium oxide, which crystallizes, is found to be a thousand times more conductive than the known yellowish brown CdO. The electrical conductivity of CdO annealed at 800 °C showed a minimum of around 88 K. It has been found very interesting by researchers that thermoelectric power generated is changed around 88 K. The X-ray diffraction pattern of the obtained yellowish brown CdO was determined to have extra lines relative to the patterns drawn after 400 or 800 °C firing (De et al. 2000).

Thirumoorthi and Prakash (2016) prepared CdO thin films with different Sn concentrations by sol-gel spin coating method. The optical band gap of CdO thin films increased from 2.42 eV to 2.96 eV. An enhanced band gap has been Burstein-Moss effect. The doping of Sn varied the parameters such as d-space, average crystallite size (D), lattice constant (a), dislocation density, strain (ϵ), thickness (nm), FWHM. The images of scanning electron microscope (SEM) revealed that the doping had a important effect on the surface. Transmittance increased in the visible region when compared to the undoped CdO thin films. From FTIR spectra of CdO thin films, the curve of transition vs. wavenumber revealed the presence of the chemical bonding and functional groups centered at 1892, 1604, 1247, 973, 663 and 551. It has been that Sn doping increases carrier concentration while it decreases the resistivity.

Gurumurugan et al. (1996) studying the optical transmittance and Hall effect of cadmium oxide thin films prepared spraying manner, the results of X-ray diffraction showed that

the thin films prepared with the installation of a multi-gelling had cube type and value of the energy gap (2.6 eV).

The researchers studied the optical properties of the membranes dioxide, cadmium and zinc oxide and prepared in a manner deposition chemical gases. They considered economic ways and optimal methods for solutions of salts, minerals, and the membranes resulting appropriate scientific studies and technological applications. After obtaining membranes they studied the optical properties such as optical energy gap, absorption coefficient, refractive index, in addition to the lattice constant of article account (Benraimane et al. 1997).

The researcher used cadmium oxide material to get the membranes dioxide, thin films of CdO, have been deposited on the substrate of the glass at 250 °C. The study shows the results of X-ray diffraction that the membrane is a substance dioxide, cadmium and installed a multi-gelling, especially when the directivity (111), fixed with a lattice of 4.96 Angstrom), and the optical properties have earned a researcher at the highest permeability in the visible and infrared regions, that the optical energy gap ranged (2.4 ±0.05) eV (Eze 1998).

Ferroaj and Rodriguez (2000), reported the optical and electrical properties of the membranes dioxide, cadmium vestiges of fluorosis and prepared a way that chemical spraying heat at temperatures (190°C, 210°C, 320°C), The results of the study showed that the impurity fluorine increased the value of the energy gap quickly and then with increasing impurity concentration and all temperatures decreased.

The researchers studied the acetate cadmium solution for the membranes dioxide, cadmium way sol-gel after deposition on glass bases and at a temperature (200-450 °C), the results of synthetic tests showed that membranes prepared multi-gelling and type cube similar to the installation of crystallizing sodium chloride and with the permeability ranging % (100-95) at wavelengths greater or equal to (600 nm) (Zuniga-Romero et al. 2001).

The researcher reported that cadmium oxide was prepared by heated and found that the interaction of impurities heated and high-temperature annealing cause a wide range of electrical conductivity (Meinhold 1987).

Hashem (1997) reported optical and electrical properties of the membranes prepared in a manner cadmium oxide chemical spraying and thermal study showed the effect of addition of chlorine and iodine impurity of cadmium oxide and different volumetric rates on optical and electrical properties of cadmium oxide membranes.



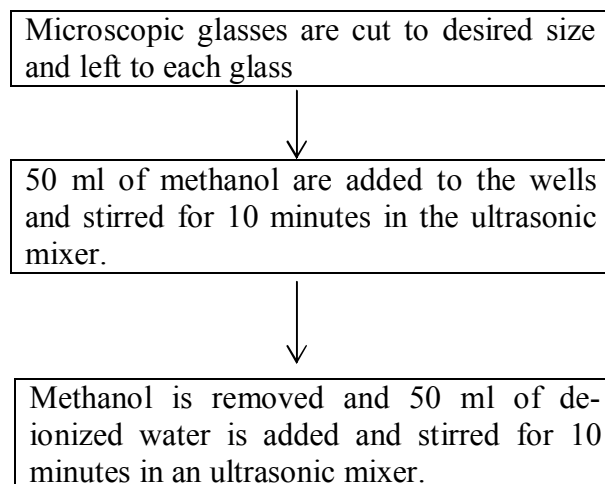
3. MATERIAL AND METHOD

3.1. Experimental Details

The cadmium acetate dehydrate ($\text{Cd}(\text{COOCH}_3)_2 \cdot 2\text{H}_2\text{O}$), ethylene glycol monomethyl ether and monoethanol amine ($\text{C}_2\text{H}_7\text{NO}$, MEA), 2-methoxyethanol ($\text{C}_3\text{H}_8\text{O}_2$) to be used to prepare CdO thin films were commercially purchased from Sigma-Aldrich Corporation. In order to prepare CdO thin films, sol-gel spin coating technique was used. The process steps are as follows:

- First, the complex compound $\text{Cd}(\text{COOCH}_3)_2 \cdot 2\text{H}_2\text{O}$ (cadmium acetate dehydrate) was dissolved in 2-methoxyethanol. Monoethanolamine was used as a stabilizer in the solution.
- The molar ratio of the stabilizer used is assumed to be 0.5.
- The resulting mixture was stirred at 60°C for 2 hours in a magnetic stirrer.
- By this process, clear and homogeneous solutions were obtained.
- The resulting solution was allowed to rest for 18 hours.

The chemical cleaning steps of the glass substrates to be used for forming CdO films are shown below.



↓

The deionized water is removed and filled with 50 ml of acetone and stirred in the ultrasonic mixer for 10 minutes.

↓

The acetone in the each glass is emptied and the microscope glasses are dried with nitrogen gas.

So, the chemical cleaning of glass bases was completed and ready for CdO coating. The process steps are as follows:

- The glass base was placed on the spin coater (Fig. 3.1).
- 2-3 drops (approximately) of the prepared jelly were dropped onto the glass.
- The spin coater is set to 30 rpm, 1000 rpm. Homogeneous and thin layer of solution were provided on the glass substrate.
- After each coating, the films were dried by heat treatment on a hot plate for 5 minutes on a table at a temperature of 150 ° C.
- These procedures were repeated 10 times for each sample. Finally, the films were annealed at 400 °C for 1 hour in the oven and cooled to room temperature.

It was aimed to purify the thin films as much as possible with the annealing process. The basic steps of the sol-gel process are shown in Fig. 3.2.



Fig 3.1. Spin coating system

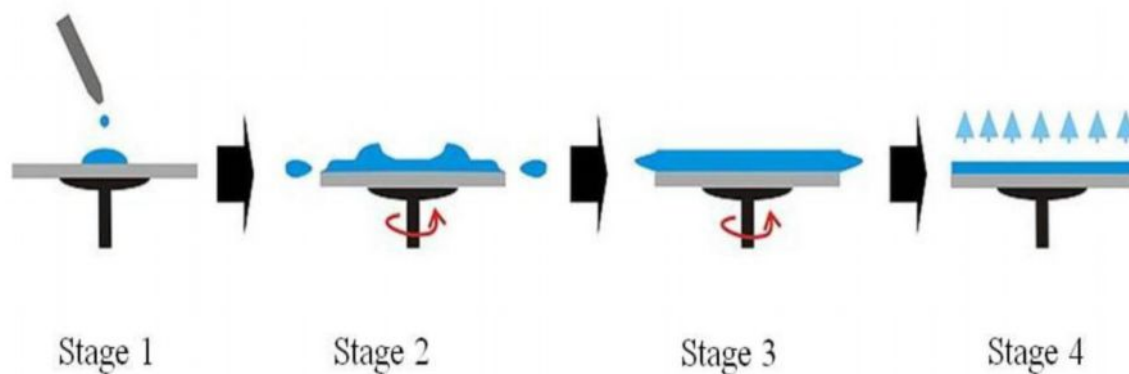


Fig 3.2. The basic steps of the sol-gel process

The morphology of the resulting thin films was examined by atomic force microscopy (AFM). Optical characterization was performed by UV-vis spectroscopy (Shimadzu UV-VISNIR3600 spectrometer). The AFM images and optical measurements are taken by equipments shown in Fig. 3.3 and Fig. 3.4 respectively.

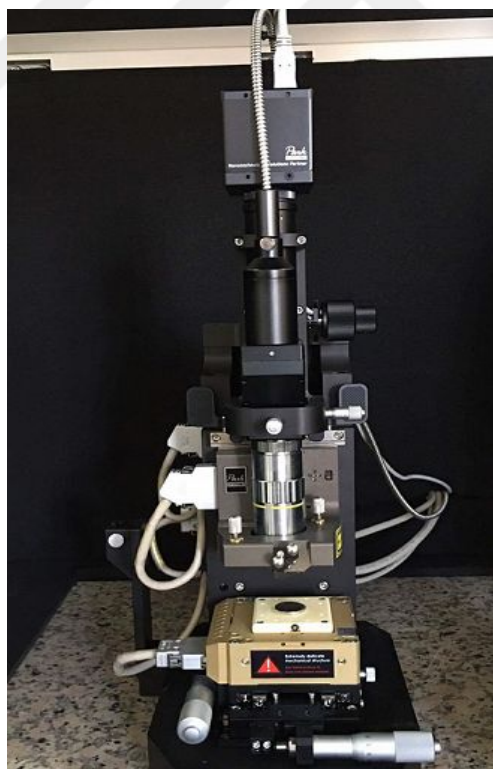


Fig 3.3. Atomic force microscope (AFM)



Fig 3.4. UV-vis spectrophotometer

The X-ray diffraction (XRD) system was used for the structural analysis (Fig. 3.5) For the application, heterojunction with CdO, which is a semiconductor surface were made. For this, one face-polished p-type silicon with a $0.01 \Omega\text{-cm}$ resistivity growth in the (100) direction was used. The process steps are as follows:

- P-type Si was cleaned by standard chemical cleaning procedure.
- To form an ohmic contact, Al layer with a thickness of 90 nm was coated by a thermal evaporator under vacuum of 3×10^{-6} torr on the back mat surface of p-Si the sample with ohmic contact was annealed at $570 \text{ }^\circ\text{C}$ in a nitrogen atmosphere.



Fig 3.5. X-ray diffraction (XRD)

- The ohmic behavior for p-Si/Al was confirmed by linear I-V characterization.

- Prepared CdO solutions were coated on the front (bright) surface of p-type Si at 1000 rpm for 30 s by a spin coater.
- Finally, circular Al dots with a diameter of 2 mm were covered on CdO thin film coated Si samples by thermal evaporation along a molybdenum mask.
- Thus, CdO/p-Si heterojunction diodes were obtained.
- Current-voltage measurements were made using a Keithley 2400 measurement system. Light dependent current-voltage characteristics were performed under solar simulator.

3.2. Sol-gel Method

Sol-Gel, that is known as chemical solution deposition process, is wet chemical technique used widely in the areas of material science and taking into account the type of ceramic. This method is used primarily for the manufacture of materials (usually metal oxide) ranging from chemical solution which acts as an introduction to the integrated network (or gel) of either discrete particles or polymers network (El-Basioni 2013). Sol-gel process is described as "Configuring dioxide through a network of reactions polycondensation of molecular precursors in the liquid (Abu-Kmail 2013). Sol-gel processes offers advantages such as low temperature curing with high homogeneity and purity of materials enable the preparation of hybrid materials and the inclusion of medicinal materials or even cells.

3.3. Thin Film Applications

The thin film is a layer (monolayer) of material ranging from fractions of a nanometer to several micrometers in thickness. Semiconductor and electronics, optical and coating are the key applications that take advantage of the construction of a thin layer (El-Basioni 2013). Thin films may include a large group thickness, varying from a few nanometers to tens of micrometers, and thus it is determined best in terms of production processes rather than fish (Oleksiyi 2008). Common methods for the production of thin films today: sputtering techniques, various chemical vapor deposition methods, sol-gel technology. The last synthesis technique has the advantages of being relatively inexpensive, can be applied at lower temperatures somewhat, and does not require expensive high vacuum equipment (Söderlind 2008).

Thin films of many practical applications can be classified in general to:

1. Electronic applications:

The use of thin-film circles in the opening and closings, rectifiers, detectors, transistors, solar cells, and amplifiers. As well as used in magnetic memory devices and integrated circuits.

2- Optical applications:

The use of thin-film interference processes utilized in photography and copiers process (Lover 1972 , Eckcrtova 1977). It has also been used in optical filters, which in turn includes the design of the mirrors and filters peremptory anti-reflection industry (Rashid 1996).

The thin film is a layer or multiple layers of materials, ranging from parts of a nanometer (monolayer) to several micrometers in thickness. Semiconductor and electronics, optical and coating are the key applications that benefit from the construction of a thin layer.

The thickness of the polymer depends on various factors:

- Solution concentration and viscosity.
- Solvent evaporation rate.
- Rotational speed.
- Running time (Bolbol 2013).

Common methods for the production of thin films today: sputtering techniques, various chemical vapor deposition methods, sol-gel technology. The last synthesis technique has the advantages of being relatively inexpensive, application at lower temperatures somewhat, and does not require expensive high vacuum equipment (Söderlind 2008).

3.4. Silicon

Silicon is the most abundant of all non-metallic elements on the ground. Progress in chemistry from this element was quickly in the past few decades. Infusibility of silicon and general compounds and resistant to attack by chemical reagents slowed significantly in the development of the chemistry of silicon until the discovery of hydrofluoric acid. At the present time, but the great, interest theoretical and practical relevance of silicon cannot be overstated (Singh and Pandey 1968).

3.5. X-ray Diffraction

X-ray diffraction (XRD) is a technique used to characterize the crystal structure, grain size, preferred orientation in the crystalline samples. This is based on the diffraction of waves by the lattice. Crystal diffracts X-rays that pass through the production of beams in a specific beam angle, depending on the wavelength of X-rays, orientation and crystal. Reflecting condition is described in the Bragg law. A beam of X-rays hits the sample interaction with the crystal planes creating a diffraction pattern for constructive interactions that meet Bragg's Law. Bragg's Law: $(n\lambda=2d\sin\theta)$. Where n is the diffraction, λ is the wavelength of the X-ray, d is the interplanar spacing of the crystal planes, and θ is the angle of the incident X-rays (Lugo 2010). The use of X-ray diffraction is a stage to identify in thin films.

3.6. Atomic Force Microscopy (AFM)

Atomic force microscope (AFM) is a tool used to describe the topology of the surface morphology of thin films. It consists of a cantilever with a sharp tip at the end used to scan the sample surface (Lugo 2010). AFM is one of the microscopic scanning probe techniques, developed by Binnig, Quate and Gerber in 1986. In AFM, the image is produced by measuring the forces of attraction or repulsive between the scanning probe tip and the surface of the sample. AFM can be used not only for topographic mapping surfaces but also can serve as a current, chemical, physical and biological sensors (Shafiei 2010).

3.7. Optical Properties

Transmittance is a measurement of how much light passes through a substance. The higher the amount of light that passes through, the larger the transmittance. Transmittance is defined as the ratio of the intensity of incident light: intensity of transmitted light. If the intensity of incident light is I_0 and the intensity of transmitted light is I , then $T=I/I_0$. At times, this fraction may be represented as a percentage, where it is called the percentage transmittance ($\%T$) (<http://pediaa.com/difference-between-absorbance-and-transmittance>) Permeability of the surface of the material to be effective in radiant energy transfer (<https://en.wikipedia.org/wiki/Transmittance>).

The energy difference between the valence E_v and the conductivity bands E_c is related to the band gap E_g . Absorbance (A) is defined as:

$$A = \log_{10} \left(\frac{1}{T} \right) \quad (3.1)$$

Consequently, the absorbance can also be given in terms of the percentage transmittance:

$$A = 2 - \log_{10} (\%T) \quad (3.2)$$

According to Beer-Lambert law, the absorbance of light, as it passes through a solution, is directly proportional to the path length of light through the material (l) and the concentration (c). So, we can write,

$$A = \epsilon lc \quad (3.3)$$

Where ϵ is a constant and called the molar absorptivity. This constant has a specific value for a given substance, providing the temperature of the substance and the wavelength of light passed through it are kept unchanged. This is an extremely useful relationship which allows concentrations of unknown solutions to be found by measuring the absorbance of light through a sample. If we make the sample solution, allow light to pass through it and plot how the transmittance changes as we change the concentration of the solution (while keeping the path length travelled by light unchanged), we get an exponential relationship between transmittance and concentration (<http://pediaa.com/difference-between-absorbance-and-transmittance>).

Reflectivity is a measure used in the field of optical measurement and heat transfer to find out radiation counter the proportion of radiation among the fallen. The reflectivity of the electromagnetic beam is not constant at each frequency but is governed by a factor of reflection and radiation frequency. In the case of the detector, it should send the beam on one frequency so as to be reflectivity largest as possible to doing his duty to the fullest, it is sent detector beam at a frequency of a reflexive slim, it will not fall back towards the

detector only a few rays that probably is not enough to give the correct information. The reflectivity by the reflectivity coefficient can be calculated:

$$\rho = \frac{\rho_r}{\rho_i} \quad (3.4)$$

Where: $\rho_i(\lambda)$: is the ability of the fallen in watts, $\rho_r(\lambda)$: is the ability of reflected beam in watts, ρ : coefficient of reflectivity (<https://en.wikipedia.org/wiki/Reflectance>).

3.8. Photoluminescence (PL)

Photoluminescence (PL) is a useful procedure for the rapid characterization in the line of materials, especially the materials needed for PV relatively new. Basic information such as the electronic band gap PL, the minority carrier lifetime, on half the Fermi level of the division can be extracted from PL measurements. (Bermel et al. 2014).

3.9. Metal-Semiconductor (MS) contacts

Usually it is used two types of semiconductor metal contact and integrated circuits manufacturing. They are Schottky and ohmic contact. Schottky barrier contact exhibits asymmetrical (I-V) characteristic when the polarity of the bias voltage is applied to metal connector and semiconductor. Ohmic contact, on the other hand, shows a linear I-V characteristic, regardless of the polarity of the external bias voltage. (Sheng 2005).

The energy difference in Fig. 3.6 is given as $\Phi = W - E_F$ and at $T = 0$ represents the minimum energy required to drive an electron out of the metal. Thus, the minimum quantum energy, hf_{\min} required to obtain the photoemission is determined. Energy determines the condition for an electron to get rid of metal. For this reason, the condition of getting rid of the surface for electrons is given to be $\frac{1}{2}(mv_x^2) \geq W$.

The term "ohmic contact is used," usually to refer to the names determined by the voltage characteristics of the resistance of a semiconductor current. Substance or device to which they belong behavior, not by communications properties themselves. The ideal contact resistance is negligible compared to that of the semiconductor material (Krämer 2000). There is a need for resistance to establish links between any semiconductor device or

Integrated circuits and the outside world. Moreover, high quality ohmic contact is necessary to perform very precise measurements (Krämer 2000).

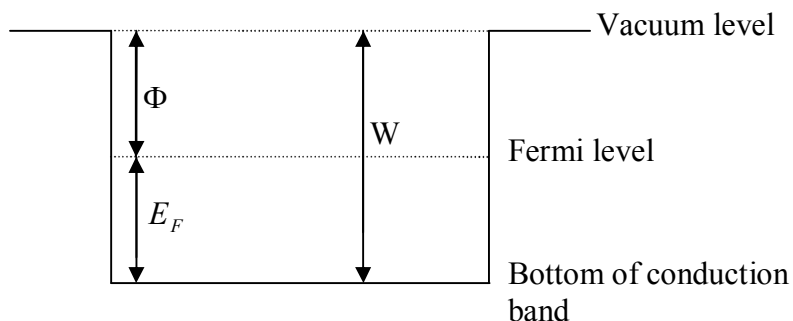


Fig 3.6. Energy level diagram of a metal

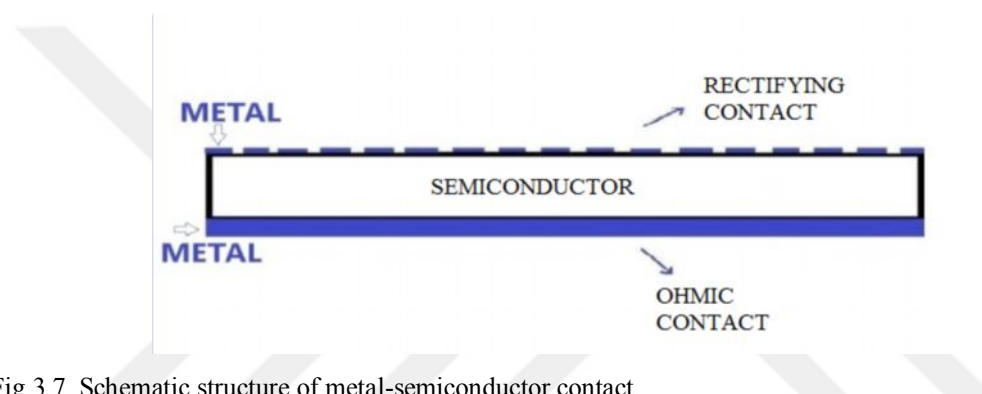


Fig 3.7. Schematic structure of metal-semiconductor contact

Quantities such as vacuum level, work function and Fermi energy are effective on barrier height. Fermi energy is called the energy of the highest full level occupied by electrons in the metal at an absolute zero temperature from the base state and is shown as E_f . It is given by the Fermi distribution function which is shown by the possibility of having the energy level of electrons in a metal at T temperature:

$$f(E) = \left\{ 1 + \exp \left[\frac{-(E_F - E)}{kT} \right] \right\}^{-1} \quad (3.5)$$

Where T is the temperature of the metal, E is the energy level at which the particle can be found, E_f Fermi energy and k Boltzman constant.

If the work function of the semiconductor is greater than the metal work function ($\Phi_m < \Phi_s$), a rectifier contact occurs. Before the contact is formed, the Fermi level of the

semiconducting metal is below the Fermi level $\Phi_m - \Phi_s$. After contact, the electrons flow toward the semiconductor side by the metal as much as the Fermi levels at the same level. As a result, the surface layer of the semiconductor is loaded negatively.

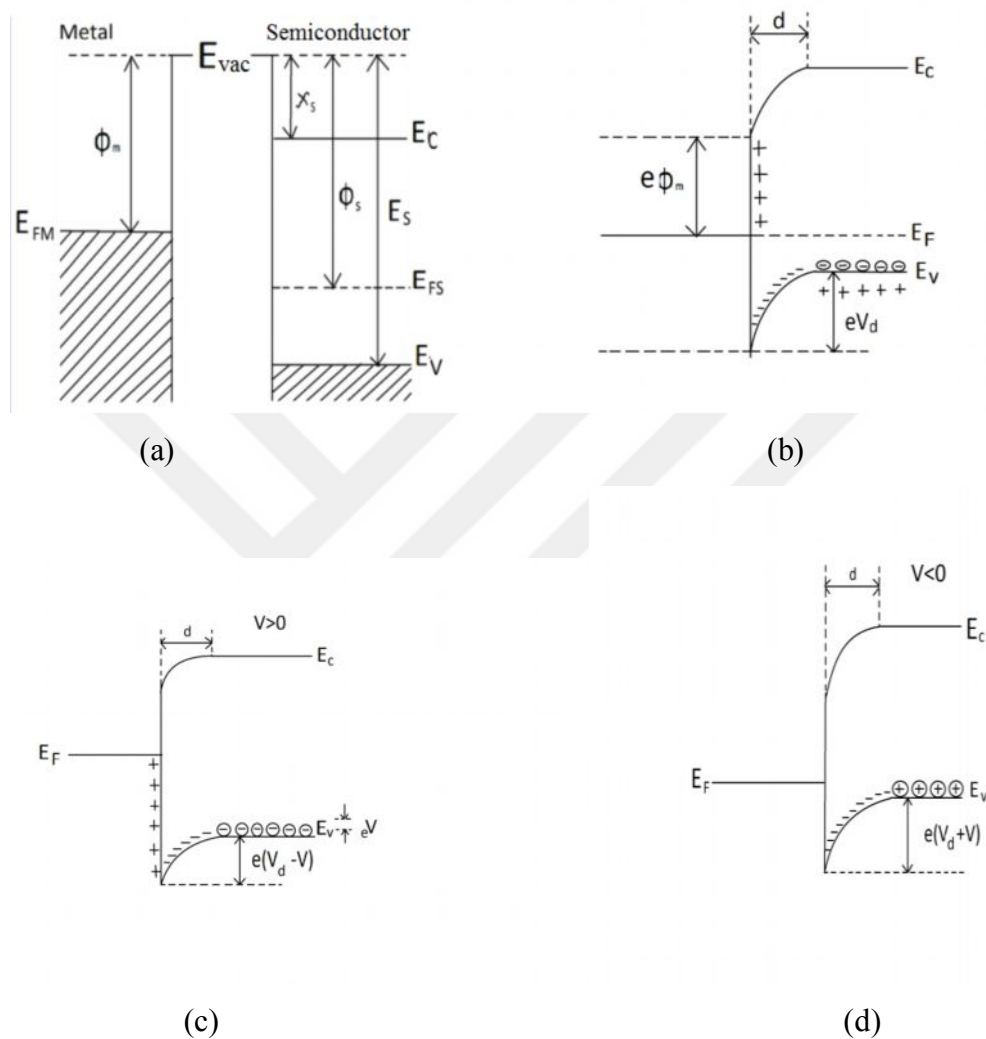


Fig 3.8. The energy-band diagram of Metal/p-type semiconductor rectifier contact (Bozkurt 2009)

- a) Before the contact
 b) After contact and in thermal equilibrium
 c) If the potential differs from zero ($V > 0$)
 d) $V < 0$

Ohmic contact: By examining the state of the metal/p-type semiconductor contact $\Phi_m > \Phi_s$; It can be seen that the Fermi level of the semiconductor is up to $\Phi_m - \Phi_s$ from the Fermi level of the metal. After the contact is made, charge exchange will take place. The electron on the semiconductor side will leave a positive surface charge behind it, and the negative surface on the metal side will flow to the side of the metal bringing the charge to

the field. As a result, the Fermi level in the semiconductor will go down by $\Phi_m - \Phi_s$ as in Fig. 3.9b. In this case, the hole concentration will increase. Accordingly, it is seen that the semiconductor surface is mostly p-type. The electrons can easily pass by the metal on the semiconductor side. Such a charge motion will correspond to the flow from semiconductors to the metal of the holes. Holes passing through the metal side are immediately neutralized. In the case of reverse bias, the thermally formed holes on the side where the metal is located can also be easily moved to the semiconducting side. In this way, a contact, i.e. an ohmic contact, which can easily pass the current from both sides will be obtained (Temirci 2001).

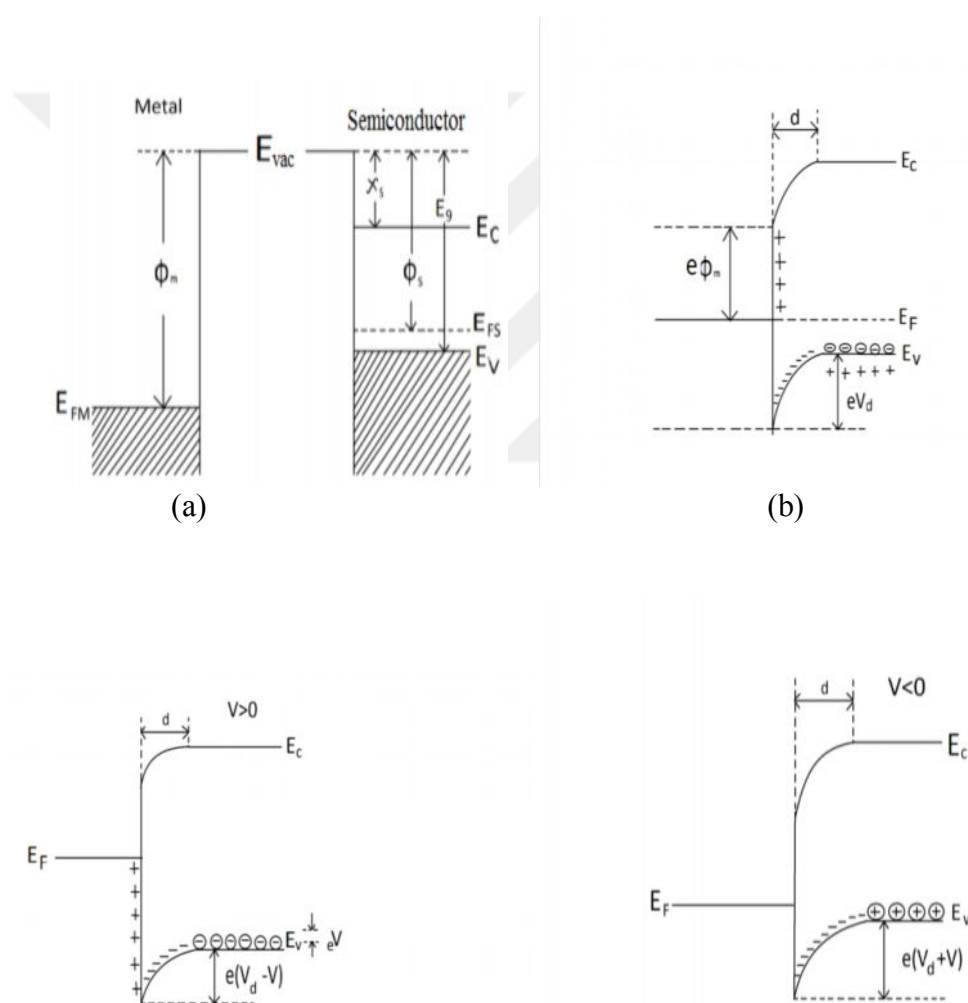


Fig 3.9. Metal/p-type semiconductor ohmic contact energy-band diagrams (Bozkurt 2009)

- a) Before the contact
- b) Next state of contact
- c) in the case of $V > 0$
- d) in the case of $V < 0$

The negative charge occurs with ionized acceptors. The resulting load is distributed along a thick space charge region. Energy levels in the semiconductor rise to:

$$\Phi_s - \Phi_m \quad (3.4)$$

Therefore, the surface barrier formed for the holes on the semiconductor side:

$$eV_{dif} = \Phi_s - \Phi_m \quad (3.5)$$

V_{dif} is diffusion potential. This potential formed in the semiconductor is taken according to the surface of the metal. The barrier height for the horns on the metal side of the contact is different from the barrier height on the semiconductor side;

$$e\Phi_b = E_s - \Phi_m \quad (3.6)$$

The scanner is a semiconductor device link p-n junction limited to the region reverse bias. Biasing arrangement basic, construction and the symbol of the device are shown in Fig. 3.10.

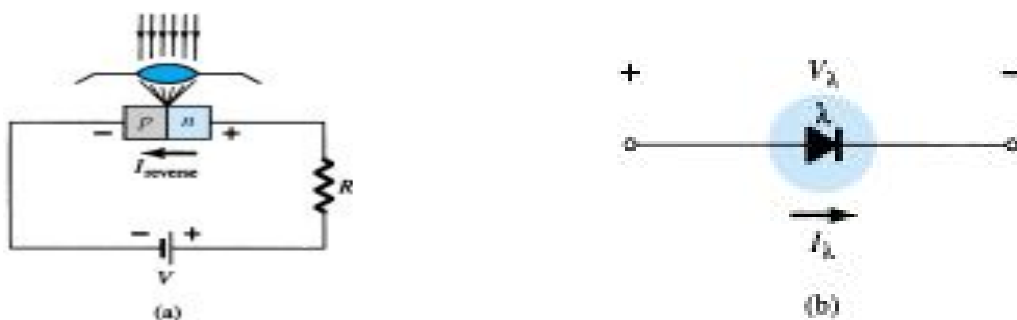


Fig 3.10. (a) basic biasing arrangement and construction; (b) symbol

Open circuit voltage (OCV or abbreviated as V_{OC}) is the difference in voltage between the stations of the device when disconnected from any department. Electric current flows between the external terminals. The potential difference mentioned in the batteries and cells is usually the open circuit voltage. The open circuit voltage is the electromotive

force, which is the maximum voltage difference when there is no current in case did not close the circle (<https://en.wikipedia.org/wiki/Open-circuit-voltage>).

PVs (Photovoltaics PV), known as solar photovoltaic cells. Are devices which the sunshine directly converts to electricity by using semiconductors such as silicon. Material of these cells either crystalline material such as crystalline silicon or amorphous thin material as amorphous silicon (Amorphous Silicon a-Si) and Cadmium (Telluride CdTe) or (Copper Indium Diselenide CuInSe₂, or CIS). It is considered as a form of renewable energies and clean energy because it is not caused by a run for contaminated waste and noise and radiation do not even need to fuel. But the cost is high compared to other primary energy sources (<https://en.wikipedia.org/wiki/Solar-cell>).

Saturation current (or current range), more precisely, the reverse saturation current, is that part of the reverse current in a semiconductor diode caused by the proliferation of minority carriers from the neutral zones to the depletion region. This current is almost independent of the reverse voltage. I_s , the reverse bias saturation current for an ideal diode, is given by

$$I = I_0 \exp\left(\frac{qV_d}{nkT}\right) \left[1 - \exp\left(\frac{-qV_d}{kT}\right) \right] \quad (3.7)$$

I_0 ; in current equation:

$$I_0 = AA^*T^2 \exp\left(-\frac{q\phi_b}{kT}\right) \quad (3.8)$$

Where q is elementary charge, A is the cross-sectional area. I is the diode current, I_s is the reverse bias saturation current (or scale current), V_D is the voltage across the diode, V_T is the thermal voltage, kT/q . n is the ideal factor, As well it is known as the quality factor. The barrier height can be calculated.

$$\ln\left(\frac{J_0}{T^2}\right) = \ln A^* - \frac{q\Phi_{b0}}{kT} \quad (3.9)$$

The plot of $\ln(J_0 / T^2)$ vs. $1/T$ gives a linearity. At 0 K, the zero-bias barrier height and Richardson constant are obtained from the value of the slope and ordinate axis of the fitted line, respectively (<https://en.wikipedia.org/wiki/Saturation-current>).

Fill factor (solar cells), the ratio of the maximum power that can be obtained for the product of open circuit voltage and short circuit current (<https://en.wikipedia.org/wiki/Fill-factor>). Energy efficiency (physics), the ratio between the useful output and input of an energy conversion process. Electrical efficiency, useful power output per electrical power consumed. Thermal efficiency, the extent to which the energy added by heat is converted to network output. Luminous efficiency, a measure of how well a light source produces visible light. Fuel efficiency, the efficiency of converting potential energy in a fuel into kinetic energy (<https://en.wikipedia.org/wiki/Energy-efficiency>).

The ideal factor (n), related to recombination in the space charge region sites. A diode that is free from defects has the ideal factor 1. As the number of defects rises (i.e doping with gold), the diodes ideality factor tends towards 2. This value is not related to the type of material used. What is important, and intrinsic to the material, is its bandgap energy. This is the energy required to jump from the valence to conduction bands. It's 1.11eV for silicon and 0.67eV for germanium (<https://www.physicsforums.com/threads/the-ideality-factor-of-silicon-and-germanium>). Norde function is given as follows:

$$F(V) = \frac{V}{\xi} - \frac{1}{\beta} \ln\left(\frac{I}{AR^*T^2}\right) \quad (3.8)$$

In Norde equation, q/kT value is described as β . Furthermore, if the parameter is accepted as $V_d \geq \frac{KT}{q}$ the expression is written as:

$$F(V) = \phi_b + IR_s - \frac{1}{2}V \quad (3.9)$$

Because in the ideal case there would be no series resistance, R_s becomes zero. In the case of only resistance, the equation of Norde (1979) becomes the following.

$$F(V) = \frac{V}{\xi} - \frac{1}{\beta} \ln\left(\frac{I}{AR^*T^2}\right) \quad (3.10)$$



4. RESULT AND DISCUSSION

4.1. Structure, Surface and Optic Properties

X-ray diffraction (XRD) is important technique to determine the structural characterization of the thin films. X-ray diffraction pattern of undoped CdO thin films is shown in Fig. 4.1 The International Centre for Diffraction Data (ICDD) collects a database related to the powder diffraction patterns. According to this database, the diffraction has the card number of the joint committee on powder diffraction standards (JCPDS): 05-0640a with cubic structure. The peak intensity of plane (111) is the highest while the plane (220) has minimum peak intensity.

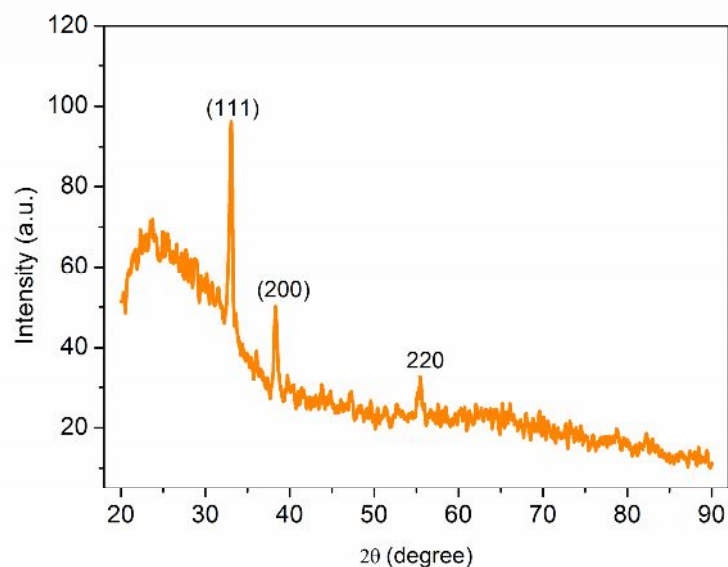


Fig 4.1. XRD spectra of CdO thin film growth on glass substrate

The lattice constant (a) is a measure of physical dimension of crystal in unit cell. The lattice constant characterizes the crystal structure and is calculated using some parameters. The related equation is as follows:

$$\frac{1}{d_{hkl}^2} = \frac{4}{3} \left(\frac{h^2 + k^2 + hk}{a^2} \right) + \frac{l^2}{c^2} \quad (4.1)$$

where d_{hkl} is interplanar spacing for planes and (hkl) is Miller indices. The value of lattice constant obtained for the dominant peak of CdO thin film is given in Table I. The lattice constant of 4.69 °A (Angstrom) determined exhibits a good agreement with the reported values (Wyckoff 1963, Wang et al. 2016). Texture coefficients, ($TC_{(hkl)}$), which are defined as the preferential orientation of crystallographic planes, are expressed by the equation (Benhaoua et al. 2014):

$$TC_{(hkl)} = \frac{I_{(hkl)} / I_{0(hkl)}}{N^{-1} \sum_N I_{(hkl)} / I_{0(hkl)}} \quad (4.2)$$

where N the number of reflections, $I_{0(hkl)}$ the standard intensity and $I_{(hkl)}$ is the relative intensity of the plane (hkl) . The texture coefficients of the diffraction peaks (111) and (200) for CdO thin films are summarized in Table I. The value of $TC_{(111)}$ is great in comparison with $TC_{(200)}$. The higher value of $TC_{(111)}$ implies low-energy crystallographic plane. The particle size (D) is expressed as (Ghosh et al. 2004, Murali et al. 2010):

$$D = \frac{0.94\lambda}{B \cos\theta} \quad (4.3)$$

where λ is the wavelength, B is the full width at half maximum (FWHM) value and θ is the Bragg angle. The value of the average crystallite size (D) was determined to be 35.02 nm (Table 4.1). It means that CdO thin films has a good crystallinity.

Table 4.1. Some structural and optic parameters of CdO thin film

Molarity	2θ	FWHM.	Texture coefficient		Average crystallite size (D) (nm)	Lattice constant (a) (°A)	E_g (eV) (PL)	R_g (nm)
			(111)	(200)				
0.5	33.02	0.272	2.560	1.701	35.02	4.6949	2.29	116.32

Fig. 4.2 shows AFM images of CdO thin film. The surface is formed from nano-sized particles. Images exhibit homogeneously covered surfaces. Surface roughness (R_q) is related to the surface texture. The parameter of roughness was determined to be 116.32nm, collecting the raw profile data. For the device performance, smooth surfaces are important.

In order to see the optical spectra such as reflectance, absorbance and transmittance, UV/Vis spectrophotometer was used. Fig. 4.3a shows the transmittance. The film shows a transparency above 80% in the visible region. Absorbance (A) and reflectance (R) are important for the efficiency of photovoltaic applications. A and R spectra are seen in Fig. 4.3b,c. Reflectivity shows a wide peak after ~ 500 nm, changing with wavelength. Absorbance allows to calculate the optical band gap, considering the absorption edge. The equation related to the optical band gap (E_g) is given as follows (Mott and Gurney 1940) :

$$\alpha h\nu = C(h\nu - E_g)^n \quad (4.4)$$

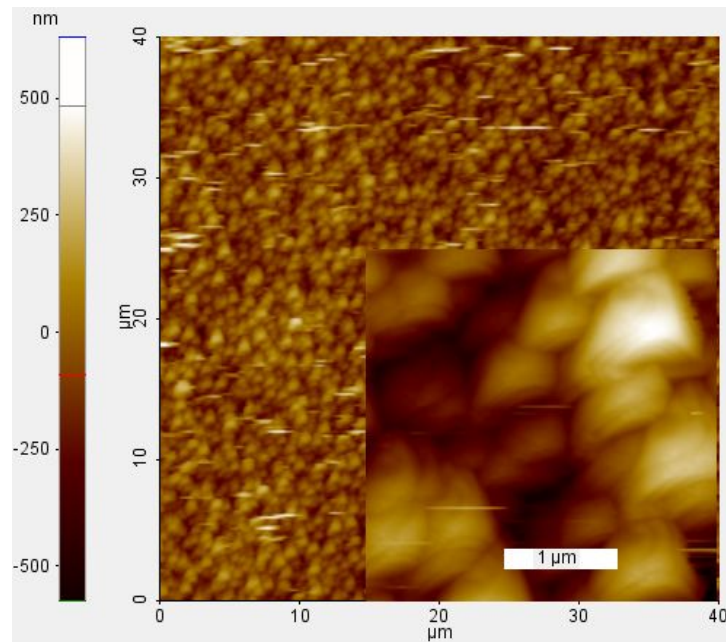


Fig 4.2. AFM microphotograph in $40 \times 40 \mu\text{m}^2$ area of CdO thin film (inset shows the image of $5 \times 5 \mu\text{m}^2$ area)

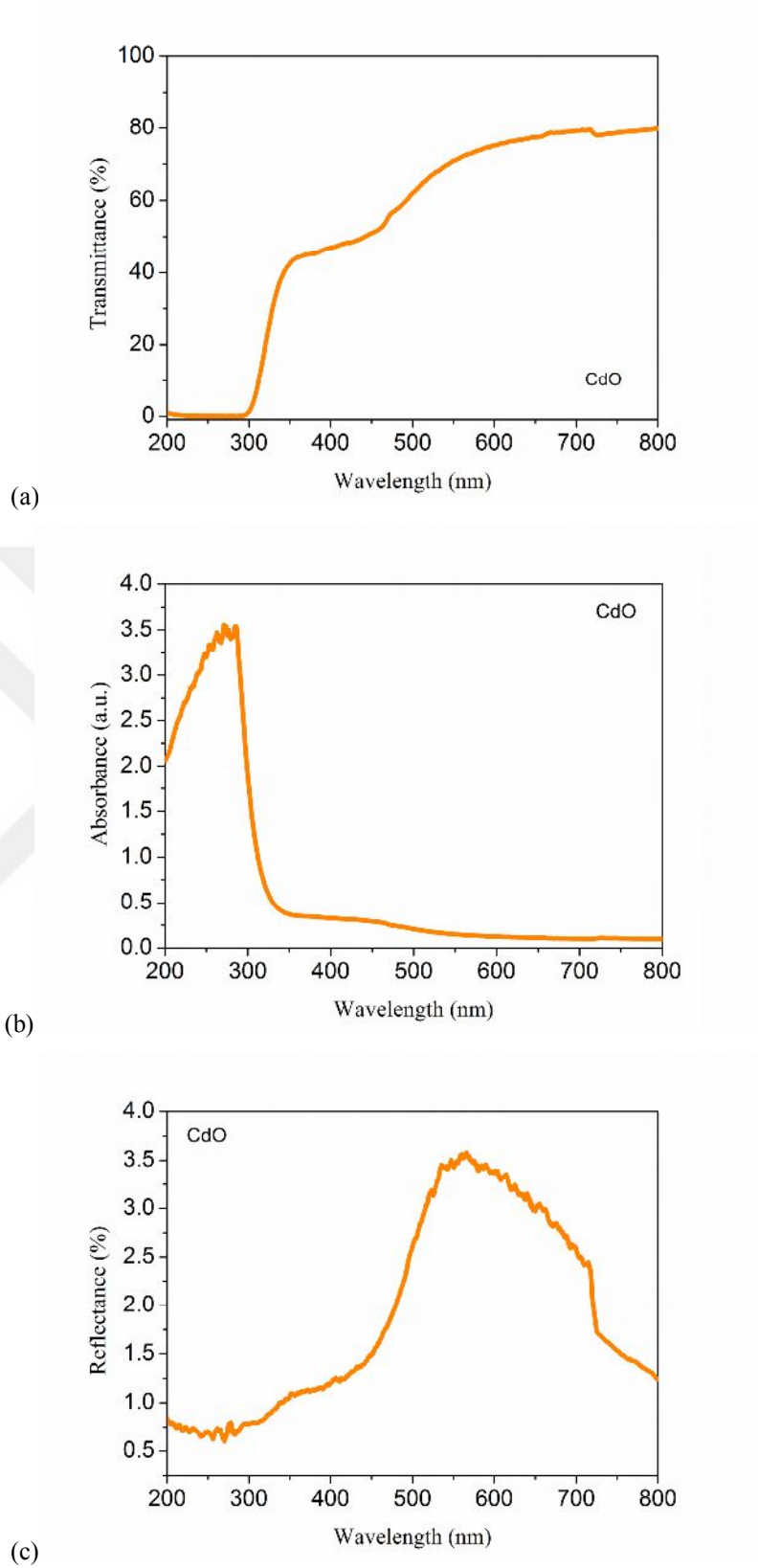


Fig 4.3. (a) Transmittance, (b) absorbance and (c) reflectance spectra of CdO thin films

where $h\nu$ the photon energy, C is a constant coefficient, α is the absorption coefficient and E_g is the optical band gap n is the transition coefficient. Fig. 4.4 shows the variation of $(\alpha h\nu)^2$ vs. $h\nu$ of the CdO films. The extrapolation of plot of $(\alpha h\nu)^2$ vs. $h\nu$ yields a linear portion. The optical band gap can be determined from the intercept of the line. According to this, the E_g value of 2.29 eV was found. The band gap of the semiconductor is also characterized by the photoluminescence spectroscopy (Eliseev et al. 2000). Fig. 4.5 shows the variation of photoluminescence (PL) intensity vs. wavelength for undoped CdO thin films. The position of the peak of CdO is dependent on the excitation wavelength of 325 nm. The band gap value using PL measurement was found to be 2.23 eV. Note that the band gap is lower than that of optical absorption spectra (Table 4.1).

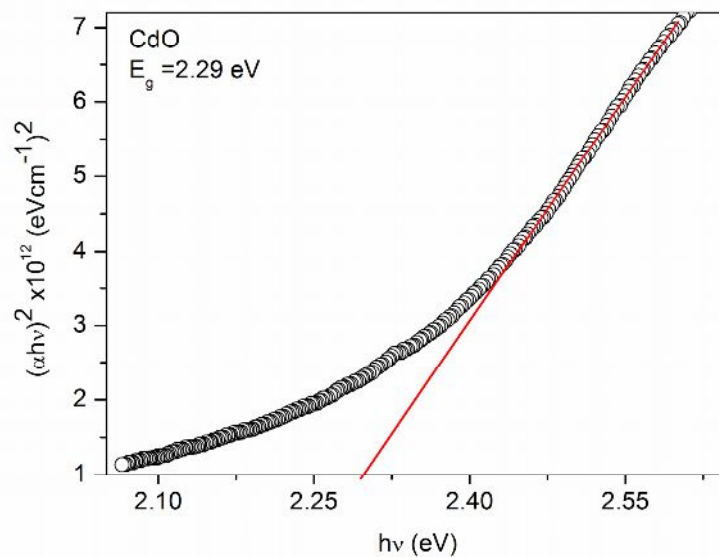


Fig 4.4. Plot of $(\alpha h\nu)^2$ vs. $h\nu$ for CdO thin films

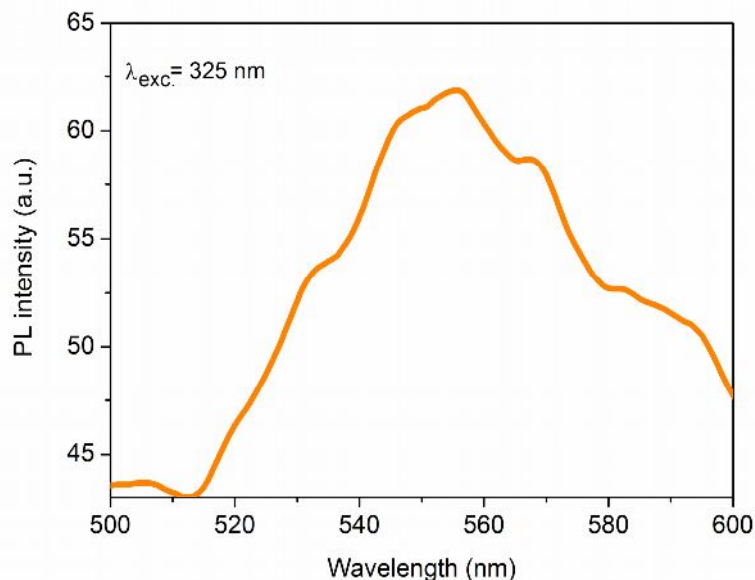


Fig 4.5. PL spectra for CdO thin films

4.2. Electrical Characteristics of CdO/p-Si Heterojunction

Anderson model used in physics to determine energy band diagram of the heterojunction can be used to describe the energy level for CdO and Si semiconductor materials (Milnes and Feucht 1972). The schematic energy band diagram of the CdO/p-Si p-n junction is seen in Fig. 4.6. According to this diagram, $\chi(\text{Si})=4.05$ eV, $\chi(\text{CdO})=4.51$ eV, $E_g(\text{CdO})=2.29$ eV and $E_g(\text{Si})=1.12$ eV (Makori et al. 2014). χ is expressed as the electron affinity. Here, the difference between the electron affinities of semiconductors is described as the conduction-band offset (ΔE_C) and the valance-band offset (ΔE_V). ΔE_C was found to be 0.46 eV [$\chi(\text{CdO})-\chi(\text{Si})$]. ΔE_V was found to be 1.63 eV [$E_g(\text{CdO})-E_g(\text{Si})+\Delta E_C$]. It is seen that ΔE_V is higher when compared to the ΔE_C . The hole injection becomes from p-Si to CdO, while the injection of electrons becomes from CdO to p-Si. The injection of electrons is higher when compared to the hole injection. There is a small potential barrier for electrons in comparison to the holes. The work function for the Al metal is known as 4.08 eV, indicating close value to the electron affinity of the Si. If the difference between the value is about zero, conductivity shows ohmic behavior. A report was published on transparent conductive inorganic (n-ZnO)/organic (p-type PEDOT:PSS) vertical heterojunction diode (Au/PEDOT:PSS/ZnO/In). The ohmic characteristic between the Au/PEDOT and In/ZnO contact was observed from the current-voltage (I - V) characteristics (Lee et al. 2011).

The rectifying characteristics may be dependent to potential energy barrier between p-type Si and n-type CdO semiconductor layers.

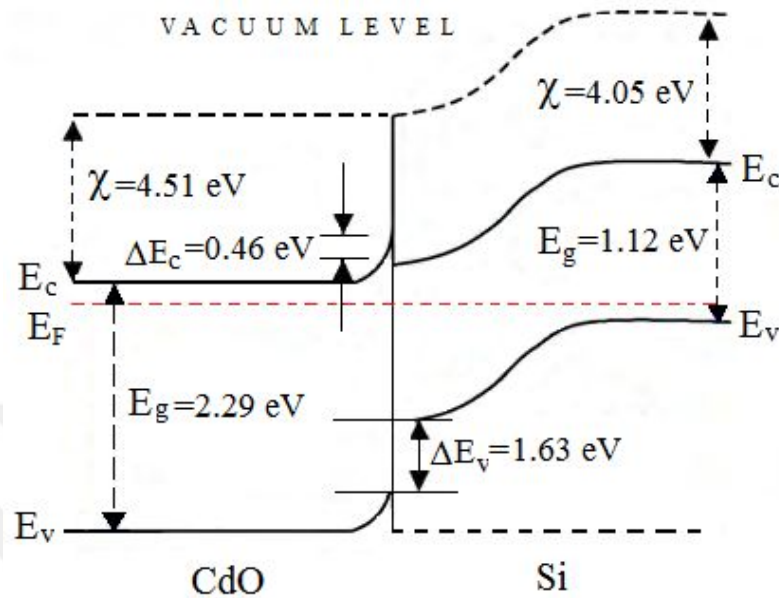


Fig 4.6. Energy band diagram of heterojunction

Junctions with upper and bottom metal contacts show ohmic behavior, indicating presence of electrons easily passing through thin films. Fig. 4.7 shows the current-voltage (I-V) characteristics of the CdO/p-Si heterojunction under dark and various illumination conditions. The reverse bias current is increasing step by step, showing a satisfying photoresponse. As the light intensity increases, the photo current increases (compared to dark condition). The ability of the single-junction photovoltaic device is observed. With incoming light, electrons are stimulated to the upper level of the band gap, and eventually an electron-hole pair is formed. Even if the band-gap energy is smaller than the incoming photon energy, the photo current increases, resulting in a coupled electron hole pair. The heterojunction with CdO thin films exhibits rectifying behavior since the forward bias current is high than that of the reverse bias. The rectification rate makes it numerical the voltage dependence of transport for the rectifying structure, The rectification ratio (RR) was found to be 8.4×10^5 at 2 V in dark condition. This value is significantly high, depending the reverse-bias leakage current of 3.91×10^{-10} A. The illumination dependence of rectification rate (RR) is summarized in Table 4.2. The turn on voltage is a measure of deviation from the ideal I - V behavior. The turn-on voltage was found to be 0.62 V.

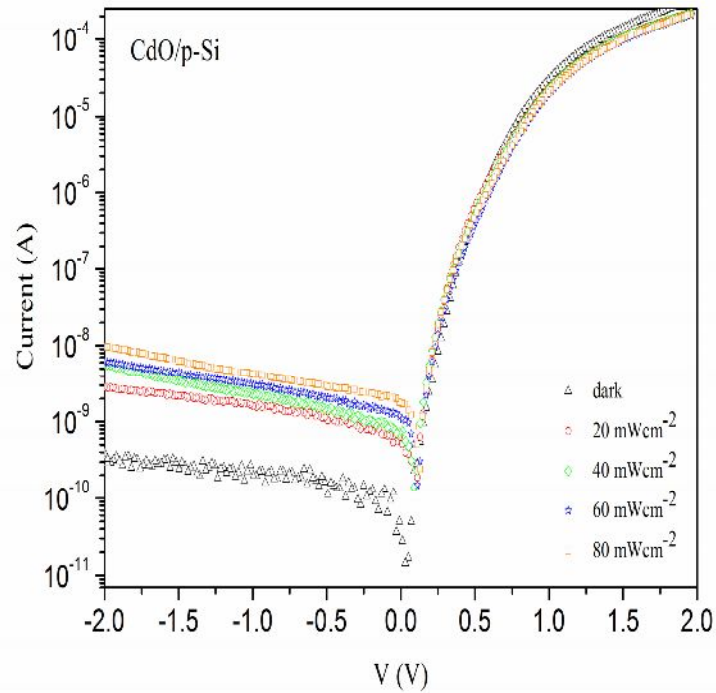


Fig 4.7. The forward and reverse bias semi-logarithmic I - V characteristics of Al/CdO/p-Si heterojunction diode in dark and under various illumination intensities

According to thermionic emission (TE) theory, the current (I)-voltage (V) relation is given as follows (Rhoderick and Williams 1988):

$$I = I_0 \exp\left(\frac{q(V - IR_s)}{nkT}\right) \quad (4.5)$$

Where I_0 is the saturation current and expressed by:

$$I_0 = AA^*T^2 \exp\left(-\frac{q\Phi_b}{kT}\right) \quad (4.6)$$

where T is the absolute temperature, q is the electronic charge, A is the effective area, V is the voltage, k is the Boltzmann constant, A^* is Richardson constant, n is the ideality factor and Φ_b is the barrier height. The slope and the intercept of the $\ln(I)$ vs. V plot

yield the ideality factor and barrier height, respectively. These values were found to be 1.43 and 1.03 eV, respectively, from dark the I - V characteristics.

The high value of the obtained barrier is about the potential barrier between the metal and the semiconductor. Ideality factor and barrier height obtained as a function of light intensity are listed in Table 4.2. The barrier height shows a linear dependence on increasing light intensity, expressing as $\Phi_{b0}(P) = \Phi_{b0} - \alpha P$ (Fig. 4.8). Where, α the illumination coefficient and P is the illumination intensity. The illumination coefficient was found to be -6.14×10^{-4} eV/W. This value is of the same order as the temperature coefficient of the band gap of the Si (-4.73×10^{-4} eV/K) (Soylu et al. 2012). Change in photo current due to barrier height and lighting intensity shows non-linear behavior. This case can be attributed to the interface states, the load resistance and the series resistance. In addition, the physical dimension of device, illumination conditions, biasing voltage, the current-limiting barrier and thermal conditions are also contributing to this change.

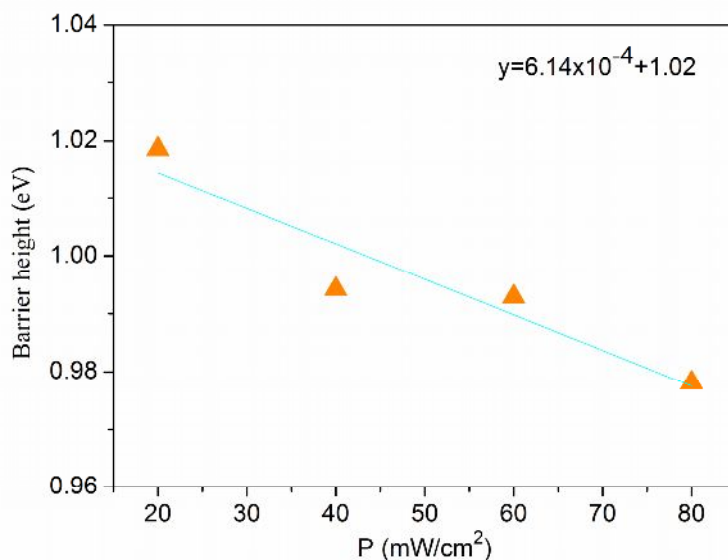


Fig 4.8. Variation of barrier height vs. P for Al/CdO/p-Si heterojunction diode

The photocurrent is given as $I_{ph} = (I_{light} - I_{dark})$. Where, I_{light} is the current measured under light and increases as the illumination intensity increases. The photocurrent is dependent on the increasing photo-generated charge carriers. The photo current obeys power law given as $I_{ph} = \kappa P^\gamma$, κ is a constant, I_{ph} is the photocurrent, and γ is an exponent (Kazim

et al. 2007). Fig. 4.9 shows the variation of I_{ph} as a function of light intensity for Al/CdO/p-Si heterojunction diode. The values of γ varied from 0.5 to 1.0. This indicates the presence of localized states, resulting in traps and defect levels due to impurities (Camaioni et al. 2000). Photons absorbed to produce photoelectron and electrons formed under dark conditions, completely create a current gain depending on the intensity of the light (Hassan et al. 2013). The current gain (g) is expressed as:

$$Gain = \frac{I_{ph}}{I_{dark}} \quad (4.7)$$

For the CdO/p-Si photodiode, the value of 30.94 was calculated at light intensity of 80 mW/cm^2 and a bias voltage of 2 V.

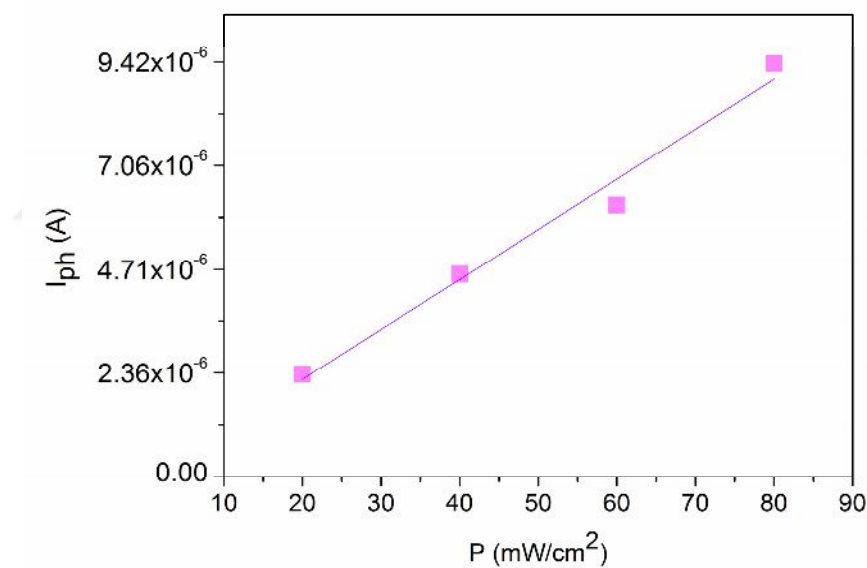


Fig 4.9. Variation of I_{ph} vs. P for Al/CdO/p-Si heterojunction diode.

There is an increased gain in the intensity of high illumination, when the trap states are saturated (Island et al. 2015).

A photo diode performance is dependent on the photo-generated charge carriers. High darkness and photo current can be obtained with improved properties of the contact components. To determine the solar cell performance of the operating device, by using a power supply as voltage source, the current density-voltage ($J-V$) characteristics were

obtained. Fig. 4.10 shows the variation of current density vs. voltage characteristics as a function of light intensity (in the range of 20, 40, 60 and 80 mW/cm²).

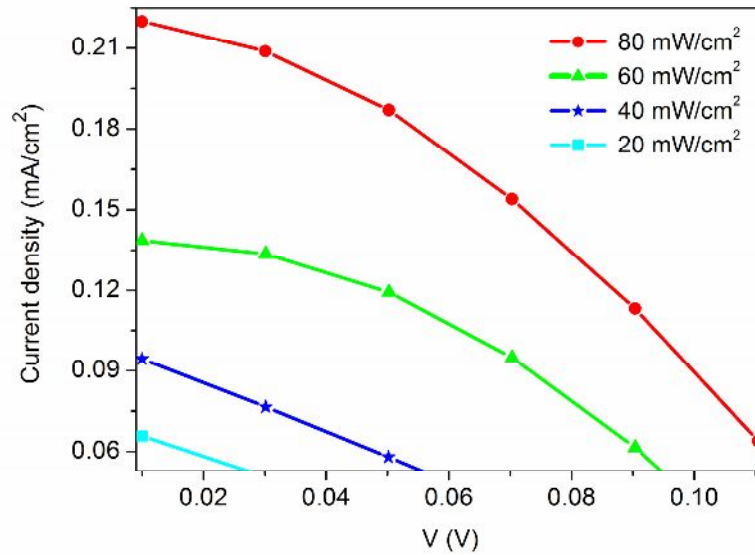


Fig 4.10. Current density-voltage characteristics at irradiance of 20, 40, 60 and 80 mW/cm²

The open-circuit voltage (V_{oc}) of a device with photovoltaic characteristics is dependent on the short circuit current density (J_{sc}) and saturation current density (J_0):

$$V_{oc} = V_T \ln\left(\frac{J_{sc}}{J_0} + 1\right) \quad (4.8)$$

where V_T is the thermal voltage at temperature of 25 °C and 25.9 mV. Photovoltaic performance indicators are given in Table 4.2.

Table 4.2. Illumination dependent values of various parameters determined from the $I-V$ characteristics of CdO/p-Si heterojunction.

Power (mW/cm ²)	Φ_b (eV)	n	RR	$R_s(\Omega)$	J_0 (mAcm ⁻²)	V_{oc} (mV)	FF %
0	1.03	1.43	8.40×10^5	1.24×10^5	1.24×10^{-8}	-	-
20	1.01	1.47	7.78×10^4	3.64×10^5	2.22×10^{-8}	28	20
40	0.99	1.60	3.81×10^4	7.94×10^5	5.73×10^{-8}	57	26
60	0.99	1.75	3.39×10^4	6.77×10^5	6.01×10^{-8}	96	34
80	0.97	1.86	2.25×10^4	1.91×10^5	1.06×10^{-7}	128	37

It is seen that the open circuit voltage (V_{oc}) increases with increasing light intensity. The value of the open circuit voltage may be insufficient for solar cell applications. However CdO thin films can be used for the development of a circuit element composed of light, sensitive components.

A model for determining photovoltaic parameters is proposed (Ortiz-Conde et al. 2006, Zhang et al. 2011, Jung and Guziewicz 2009, Dawidowski et al. 2016). The well-known Shockley equation can be used to analyze the current-voltage characteristics of this model:

$$I_0 = \left(I_{sc} + \frac{R_s I_{sc} - V_{oc}}{R_{sh}} \right) \exp\left(-\frac{qV_{oc}}{nkT} \right) \quad (4.9)$$

$$I_{ph} = I_{sc} + \frac{R_s I_{sc}}{R_{sh}} - I_0 \quad (4.10)$$

where R_{sh} is the shunt resistance, R_s is the series resistance, I_0 is the saturation current and I_{ph} is the photocurrent. Fig. 4.11 shows the plot of $I-V$ of operating device. The blue line shows the fit to the current-voltage curve. The inset shows an equivalent circuit to which the parasitic and diode resistances are added. Fitting curve makes it possible to find some parameters for the photovoltaic cell. Shunt and series resistances (R_{sh} , R_s) at the highest light intensity were found to be $1.8 \times 10^4 \Omega$ and $2.1 \times 10^5 \Omega$, respectively.

Also, Norde function $F(V)$ allows to find the series resistance. The function expressed by Norde (Norde 1979) is:

$$F(V) = \frac{V_0}{\xi} - \frac{kT}{q} \left(\frac{I(V)}{A^* AT^2} \right) \quad (4.11)$$

where ξ is the integer greater than n and dimensionless. Fig. 4.12 shows the plots of $F(V)$ vs. voltage in dark and as function of light intensity. The barrier height and the series resistance are given as follows:

$$\Phi_b = F(V_0) + \frac{V_0}{\xi} - \frac{kT}{q} \quad (4.12)$$

$$R_s = \frac{kT(\xi - n)}{qI_o} \quad (4.13)$$

where $F(V)$ gives the minimum point expressed as $F(V_0)$. The values of R_s determined in dark and as function of light intensity are summarized in Table 4.2. There is a close agreement between the values of obtained from Norde plot and fitting to equivalent circuit model.

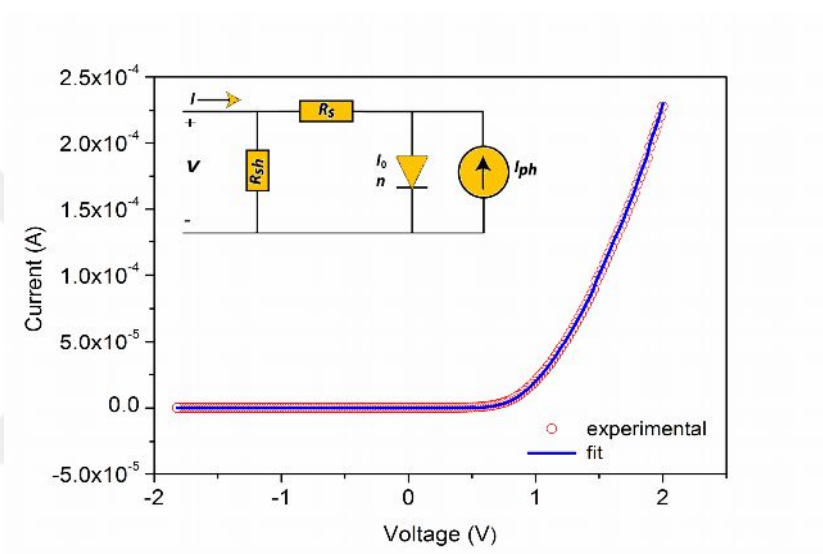


Fig 4.11. $I-V$ characteristics (open circle) with fitting curve (blue line) at irradiance of 80 mW/cm^2 (Inset shows a diode equivalent circuit of device including diode and parasitic resistances)

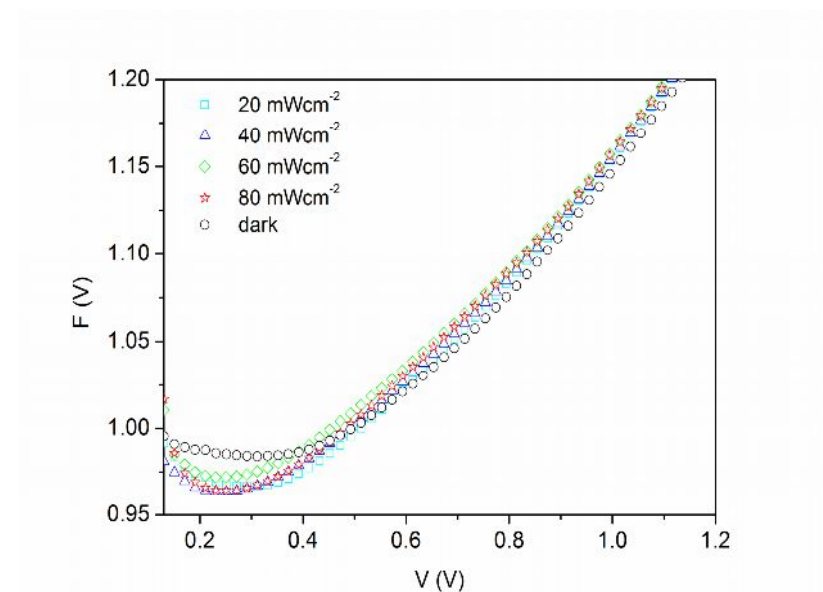


Fig 4.12. Plots of $F(V)$ vs. V

In conclusion, CdO thin films synthesized by sol–gel method exhibited crystal properties, predominantly in (111) plane. The AFM images confirmed that CdO thin films were formed from nano particles. A transparency above 80% and low reflectance in the visible region for CdO thin films were observed. The optical band gap was found to be 2.29 eV. The variation of photoluminescence (PL) intensity vs. wavelength gave a peak at about 556 nm by pointing the absorption band edge. The valence band offset (ΔE_V) was found to be higher compared with conduction band offset (ΔE_C), confirming a small potential barrier for electrons in comparison to the holes. CdO/p-Si heterojunction exhibited rectifying behavior, showing the high rectification ratio (RR) and low reverse-bias leakage current of 8.4×10^{-5} and 3.91×10^{-10} A, respectively at 2 V in dark condition. The reverse bias current was found to be increased step by step with increasing illumination intensity, indicating the photodiode behavior. The barrier height exhibited a linear dependence on increasing light intensity, allowing the determination of the lighting coefficient of -6.14×10^{-4} eV/W. The photo current varied linearly with increasing light intensity, obeying a power law. Even if the photovoltaic parameters are insufficient for solar cell applications, CdO thin films are promising for the development of a circuit element composed of light sensitive components. A model for determining photovoltaic parameters was applied to the current-voltage characteristics. The fitting curve allowed the determination of parameters such as the shunt resistance, the series resistance and the saturation current. It has been seen that there is a close agreement between the values of obtained from Norde plot and equivalent circuit model.

REFERENCES

Abu-Kmail MY (2013) Activity behavior of human serum albumin doped in silica sol-gel thin film. Master Thesis, Islamic University of Gaza, Palestine

Benhaoua B, Rahel A, Benramache S (2014) The structural, optical and electrical properties of nanocrystalline ZnO:Al thin films. *Superlattices and Microstructures* 68: 38–47

Benraïmdane N, Murad WA, Misho RH, Ziane M, Kebbab Z (1997) A chemical method for the preparation of thin films of CdO and ZnO. *Materials Chemistry and Physics* 48(2): 119–123

Bermel P, Cheng GJ, Wang X (2014) Photonic systems for crystalline silicon and thin-film photovoltaic manufacturing. Purdue University Libraries

Bolbol HZ (2013) Preparation and characterization of Iron 1,10-phenanthroline complex encapsulated in silica sol-gel derived thin films. Master Thesis, Islamic University of Gaza, Palestine

Burbano M, Scanlon DO, Watson GW (2011) Sources of conductivity and doping limits in CdO from hybrid density functional theory. *Journal of the American Chemical Society* 133(38): 15065–15072

Camaioni N, Casalbore-Miceli G, Beggiato G, Cristani M, Summonte C (2000) Photoelectrical characterization of Schottky junctions between poly(4h-cyclopenta[2,1-b:3,4-b']dithiophene) and aluminium: effect of hexadecyl groups in 4 position. *Thin Solid Films* 366(1-2): 211–215

Carballeda-Galicia DM, Castanedo-Perez R, Jimenez-sandoval O, Torres-Delgado G, and Zuniga-Romero CI (2000) High transmittance CdO thin films obtained by the sol-gel method. *Thin Solid Films* 371: 105-108

Dawidowski W, Sciana B, Lindert IZ, Mikolasek M, Bielaka K, Badura M, Pucicki D, Radziejewicz D, Kova' CJ, Tłaczała M (2016) The influence of top electrode of InGaAsN/GaAs solar cell on their electrical parameters extracted from illuminated I–V

characteristics. *Solid-State Electron* 120: 13–18

De U, Chattopadhyaya M K, Chaudhury S, Sarkar A, Sanyal D, Dey TK (2000) Electrical conductivity, thermo-electric power and structure of differently heat-treated CdO. *Journal of Physics and Chemistry of Solids* 61: 1955-1958

Eckertova L (1977) *Physics of thin films*. plenum press, New York

El-Basioni A (2013) Coated sol-gel thin films of some pH- indicators, preparation and Characterization. Master Thesis, Islamic University of Gaza, Palestine

Eliseev PG, Osinski M, Lee J, Sugahara T, Sakai S (2000) Band-tail model and temperature-induced blue-shift in photoluminescence spectra of $\text{In}_x\text{Ga}_{1-x}\text{N}$ grown on sapphire. *Journal of Electronic Materials* 29(3): 332–341

Eze FC (1998) CdO thin films synthesized by a modified reactive thermal deposition process. *Il Nuovo Cimento D* 20(9): 1421-1430

Ferroaj R, Rodriguez A (2000) Study of some optical properties of CdO:F thin films. *Physics State Solid* 220(1): 299-304

Ghosh R, Basak D, Fujihara S (2004) Effect of substrate-induced strain on the structural, electrical, and optical properties of polycrystalline ZnO thin films. *Journal of Applied Physics* 96: 2689

Gurumurugan K, Mangalaraj D, Narayandas SK (1996) Magnetron sputtered transparent conducting CdO thin films. *Journal of Electronic Materials* 25(5): 765–770

Gurumurugan K, Mangalaraj D, Narayandass SK (1995) Structural characterization of cadmium oxide thin films deposited by spray pyrolysis. *Journal of Crystal Growth* 147(3–4): 355-360

Gurumurugan K, Mangalaraj D, Naragandass SAK , Nakanisni Y (1996) DC reactive magnetron sputtered CdO thin films. *Materials Letters* 28(4–6): 307-312

Hashem EH (1997) Optical and electrical properties of cadmium oxide (CdO) thin film. Master Thesis, AL-Mustansiryia University

Hassan NK, Hashim MR, Allam NK (2013) low power UV photodetection characteristics

of cross-linked ZnO nanorods/nanotetrapods grown on silicon chip. *Sensors and Actuators A: Physical* 192: 124–129

<https://www.physicsforums.com/threads/The-ideality-factor-of-silicon-and-germanium>

<http://pediaa.com/Difference-between-absorbance-and-transmittance>

<https://en.wikipedia.org/wiki/Energy-efficiency>

<https://en.wikipedia.org/wiki/Fill-factor>

<https://en.wikipedia.org/wiki/Saturation-current>

<https://en.wikipedia.org/wiki/Transmittance>

<https://en.wikipedia.org/wiki/Reflectance>

<https://en.wikipedia.org/wiki/Open-circuit-voltage>

<https://en.wikipedia.org/wiki/Solar-cell>

Island JO, Blanter SI, Buscema M, van der Zant HSJ, Castellanos-Gomez A (2015) Gate controlled photocurrent generation mechanisms in high-gain In_2Se_3 phototransistors. *Nano Lett* 15(12): 7853

Jung W, Guziewicz M (2009) Schottky diode parameters extraction using Lambert function. *Materials Science and Engineering:B* 165(1-2): 57–59

Kazim S, Ali V, Zulfequar M, Haq MM, Husain M (2007) Electrical transport properties of poly[2-methoxy-5-(2'-ethyl hexyloxy)-1,4-phenylene vinylene] thin films doped with acridine orange dye. *Physica B: Condensed Matter* 393(1-2): 310–315

Krämer MCJCM (2000) Fabrication and characterization of metal - semiconductor contacts for application in $\text{Al}_x\text{Ga}_{1-x}\text{N}/\text{GaN}$ HEMTs. Master Thesis, technische universiteit Eindhoven

Lee DH, Park DH, Kim S, Lee SY (2011) Half wave rectification of inorganic/organic heterojunction diode at the frequency of 1 kHz. *Thin Solid Films* 519(16): 5658–5661

Li SS (1993) Semiconductor physical electronics. University of Florida

Lover KD (1972) Thin films. Imperial College, London

Lugo F (2010) Synthesis and characterization of silver doped zinc oxide thin films for optoelectronic devices. University of Florida

Makori NE, Amatalo IA, Karimi PM, Njoroge WK (2014) Optical and electrical properties of CdO: Sn thin films for solar cell applications. *International Journal of Optoelectronic Engineering* 4(1): 11-15

Mane RS, Pathan HM, Lokhande CD, Han SH, (2006) An effective use of nanocrystalline CdO thin films in dye-sensitized solar cells. *Solar Energy* 80(2): 185–190

Meinhold, RH (1987) Studies of impure cadmium oxide semiconductors using NMR, EPR and conductivity measurements. *Journal of Physics and Chemistry of Solids* 48 (10): 927—934

Milnes G, Feucht DL (1972) Heterojunctions and metal– semiconductor Junctions. New York: Academic

Mott NF Gurney RW (1940) Electronic processes in ionic crystals. Oxford University Press, London

Murali KR, Kalivanan A, Perumal S, Pillali NN (2010) Sol–gel dip coated CdO:Al films. *Journal of Alloys and Compounds* 503(2): 350–353

Norde H (1979) A modified forward I-V plot for Schottky diodes with high series resistance. *Journal of Applied Physics* 50(7): 5052

Oleksiyi L (2008) Study of thin film solar cell based on copper oxide substrate by DC reactive magnetron sputtering. Master Thesis, Universita Degli Studi Di Padova

Ortiz-Conde A, Sanchez FJG, Muci J (2006) New method to extract the model parameters of solar cells from the explicit analytic solutions of their illuminated I–V characteristics. *Solar Energy Materials and Solar Cells* 90(3): 352–361

- Phatak G, Lal R (1994) Deposition and properties of cadmium oxide films by activated reactive evaporation. *Thin Solid Films* 245(1–2): 17–26
- Rajput JK, Pathak TK, Kumar V, Kumar M (2017) L.P. purohit annealing temperature dependent investigations on nano-cauliflower like structure of CdO thin film grown by sol–gel method. *Surfaces and Interfaces* 6: 11–17
- Rashid HG (1996) Design and optimization of thin-films optical filters with applications in the visible and infrared regions. Phd. Thesis, AL-Mustansirya University
- Rhoderick EH, Williams RH (1988) *Metal–semiconductor contacts*. 2nd ed. Oxford: Clarendon Press
- Saravani C, Reddy KTR, Reddy PS, Reddy PJ (1994) Characterization of sprayed CdO thin films. *Journal of Materials Science Letters* 13(14): 1045–1047
- Shafiei M (2010) Investigation of nanostructured thin film based Schottky diodes for gas sensing applications. RMIT University
- Singh K, Pandey LP (1968) Preparation of high purity silicon. *Journal of Scientific & Industrial Research* 27(10): 386
- Sonawane NB, Baviskar PK, Ahire RR, Sankapal BR (2017) CdO necklace like nanobeads decorated with PbS nanoparticles: room temperature LPG sensor. *Materials Chemistry and Physics* 191: 168-172
- Soylu M, Al-Ghamdi AA, Yakuphanoglu F (2012) Influence of illumination intensity and temperature on the electrical characteristics of an Al/p-GaAs/In structure prepared by thermal evaporation. *Microelectronic Engineering* 99: 50–57
- Söderlind F (2008) Colloidal synthesis of metal oxide nanocrystals and thin films. Linköping University, Sweden
- Sravani C, Ramakrishna Reddy KT, Reddy PJ (1991) Physical behaviour of CdO films prepared by activated reactive evaporation. *Semiconductor Science and Technology* 6: 1036
- Taşçoğlu I, Soyly M, Altındal Ş, Al-Ghamdi AA, Yakuphanoglu F (2012) Effects of interface states and series resistance on electrical properties of Al/nanostructure CdO/p-GaAs diode. *Journal of Alloys and Compounds* 541: 462–467

Temirci C, Bati B, Sağlam M, Türüt A (2001) High-barrier height Sn/p-Si Schottky diodes with interfacial layer by anodization proces. *Applied Surface Science* 172: 1-7

Thambidurai M, Muthukumarasamy N, Ranjitha A, Velauthapillai D (2015) Structural and optical properties of Ga-doped CdO nanocrystalline thin films. *Superlattices and Microstructures* 86: 559–563

Thirumoorthia M, Prakash JTJ (2016) Effect of F doping on physical properties of (211) oriented SnO₂ thin films prepared by jet nebulizer spray pyrolysis technique. *Superlattices and Microstructures* 89: 378–389

Varkey AJ, Fort AF (1994) Transparent conducting cadmium oxide thin films prepared by a solution growth technique. *Thin Solid Films* 239(2): 211-213

Wang WJ, Xie XJ, Liu JY, Gao KH (2016) Weak localization in CdO thin films prepared by sol–gel method. *Solid State Communications* 239: 1–4

Wyckoff RWJ (1963) *Crystal structure*. 2nd Ed. New York: Wiley

Yan M, Lane M, Kannewurf CR, Chang RPH (2001) Highly conductive epitaxial CdO thin films prepared by pulsed laser deposition. *Applied Physics Letters* 78(16): 2342

Zhang C, Zhang J, Hao Y, Lin Z, Zhu C (2011) A simple and efficient solar cell parameter extraction method from a single current-voltage curve. *Journal of Applied Physics* 110(6): 064504

Zuniga-Romero CI, Torres-Delgado G, Jimenez-Sandovall S, Jimenez O, Castanedo R (2001) Influence of firing temperature on the properties of CdO thin films obtained by the sol-gel method. *Modern Physics Letters* 15(17-19): 726





CURRICULUM VITAE

I was born in February 14, 1973 in the city of Kirkuk / Iraq. Completed my elementary, middle and junior high in Kirkuk. I began to study physics at the University of Tikrit in 1993, and graduated in 1997 and got a bachelor's degree in physics. Since 2008 I worked as a teacher of physics in the city of Kirkuk. I am starting my master's in February 2015 in Bingol / Turkey University, and earned a master's degree in physics at the Feb. 2017.